small methods
www.small-methods.com

3D-Printing of Functional Biomedical Microdevices via Light- and Extrusion-Based Approaches

*Henry H. Hwang, Wei Zhu, Grace Victorine, Natalie Lawrence, and Shaochen Chen**

3D-printing is a powerful additive manufacturing tool, one that enables fabrication of biomedical devices and systems that would otherwise be challenging to create with more traditional methods such as machining or molding. Many different classes of 3D-printing technologies exist, most notably extrusion-based and light-based 3D-printers, which are popular in consumer markets, with advantages and limitations for each modality. The focus here is primarily on showcasing the ability of these 3D-printing platforms to create different types of functional biomedical microdevices—their advantages and limitations are covered with respect to other classes of 3D-printing, as well as the past, recent, and future efforts to advance the functional microdevice domain. In particular, the fabrication of micromachines/robotics, drug-delivery devices, biosensors, and microfluidics is addressed. The current challenges associated with 3D-printing of functional microdevices are also addressed, as well as future directions to improve both the printing techniques and the performance of the printed products.

1. Introduction

3D-printing technologies have made significant strides in both technological sophistication and ubiquity, with users across consumer, academic, industrial, and medical domains incorporating 3D-printing into their workflows. By "3D-printing," we refer to a wide variety of additive manufacturing processes that successively "add" material in a controlled manner, thus generally enabling the fabrication of user-defined 3D objects. This is in contrast with subtractive manufacturing and machining techniques, where the final construct is created by successively "removing" material from a solid bulk substance. 3D-printing has gained popularity due to its rapid prototyping flexibility, as well as the ability to produce features that would otherwise be challenging to produce with strictly subtractive manufacturing, i.e., nonstandard geometries, multimaterial layers, and isolated hollow spaces. In the context of creating functional microdevices, where multiple length scales and grades of complexity may be required in a quickly evolving field of biomedical needs, such 3D-printing capabilities can be invaluable.

By "functional microdevices," we refer to systems and technologies that, by way of fabrication and/or function, generally perform tasks on the microscale. These devices can vary greatly in both form and function, but in the biomedical domain they tend to serve diagnostic and/or therapeutic purposes. Examples span the range from microscale robotics and biosensors to tissue-engineered models and microfluidic lab-on-a-chip systems, with some devices capable of fulfilling more than one role. As 3D-printing technology improves, so too does the ability to fabricate functional microdevices of higher sophistication and functionality, which is of significant importance to the biomedical research, industry, and healthcare fields, as there are growing demands on improving not just the speed and cost of fabrication but also its scalability and utility.

Here, we acknowledge that there have already been extensive efforts to characterize the technical performance of most popular 3D-printing modalities, such as fused-deposition-modeling (FDM)-based, multijet-modeling (MJM)-based, and laser stereolithography (SLA). In lieu of comparing the detailed minutiae of different technical performance parameters of different 3D-printing methods, we instead direct particular focus on showcasing the different types of functional biomedical microdevices that have been created via 3D-printing, primarily light- and extrusion-based modalities. Building from previous reviews in the field of 3D-printing for biomedical applications,[1–4] we briefly discuss the basic principles of various 3D-printing paradigms, the relative advantages and limitations, and salient examples of recent and prominent functional biomedical microdevices created by 3D-printing.

2. Current 3D-Printing Technologies

On a fundamental level, 3D-printing involves successive addition of material to itself in a precise, controlled manner, ultimately resulting in a 3D object. However, in recent years, 3D-printing techniques have innovated and matured along different paths, resulting in a plethora of technologies that are capable of creating functional microdevices. Here, we describe the basic operating principles of several different 3D-printing modalities that we have loosely categorized into two overarching types: extrusion-based

H. H. Hwang, Dr. W. Zhu, G. Victorine, N. Lawrence, Dr. S. Chen
Department of NanoEngineering
University of California
San Diego, La Jolla, CA 92093, USA
E-mail: chen168@eng.ucsd.edu

The ORCID identification number(s) for the author(s) of this article can be found under https://doi.org/10.1002/smtd.201700277.

DOI: 10.1002/smtd.201700277

3D-printing (E-3DP), where there is controlled release/deposition of a material via a forming tool, and light-based 3D-printing (L-3DP), where directed light is used to selectively shape material into desired 3D constructs. While we acknowledge that not all 3D-printing modalities will fit neatly into these two classifications, they serve as a useful mental model in assessing relative advantages and limitations. A pictorial overview of the 3D-printing techniques most relevant here is given in **Figure 1**.

2.1. Extrusion-Based 3D-Printing

E-3DP covers a number of different types of 3D-printers—of them, perhaps the most common examples used in fabricating functional biomedical microdevices are FDM, nozzle-based 3D-printing, and MJM. While there are differences in the compositions of the materials used and the exact manner in which they are deposited, all fundamentally depend on the controlled release of the building material via a forming tool.

2.1.1. Fused Deposition Modeling

FDM-based 3D-printers have gained much popularity in the last decade, in part not only due to the expiry of the original patent on FDM technology in 2009 but also due to their relatively simple construction and inexpensive material costs. These types of printers additively build 3D structures by extruding thermoplastic materials via a heated, motorized nozzle that can be digitally controlled such that it translates freely in 3D-space. As the material extrudes from the nozzle, it partially cools on contact with air, thus depositing and fusing material in a line-by-line, layer-by-layer fashion until the final 3D object is formed. FDM 3D-printers are most commonly known to use thermoplastic materials primarily due to low melting temperatures, and in the context of fabricating functional biomedical devices there are many suitable plastics and polymers that are not only inexpensive, but can have desirable material properties such as biocompatibility and mechanical durability. Examples of common materials used in FDM include acrylonitrile butadiene styrene, polypropylene, polycarbonate;[7] biocompatible polymers include examples such as polycaprolactone, poly(lactic acid), and poly(glycolic acid),[8] most of which are sold in cheap, easy-to-use form factors such as pellets, wires, and laminates.

2.1.2. Nozzle-Based 3D-Printing

Nozzle-based 3D-printing is a more generalized version of FDM in that the material choices are not limited to strictly thermoplastic materials. Rather, this modality allows the use of any liquid and/or flowable precursors that can be driven through a nozzle; these precursors can be immobilized and/or removed as necessary to build the final structure (again in a drop-by-drop, line-by-line, layer-by-layer fashion). Thus, in comparison to FDM, users are afforded more material choices in fabricating functional microdevices, and examples can range from colloidal nanoparticles and cell-laden solutions to hydrogels and viscoelastic materials. This approach is particularly suited for bioprinting applications, where soft, biocompatible materials that would otherwise be incompatible with FDM techniques are used in fabricating structures meant for biological interaction.

2.1.3. Multijet Modeling

MJM, otherwise known more generically as inkjet 3D-printing, operates in a manner similar to the inkjet printers commonly seen in consumer and business environments—liquid droplets

Henry H. Hwang is a Ph.D. student at the University of California, San Diego in the Department of NanoEngineering working under Dr. Shaochen Chen. He received his B.S.E in biomedical engineering at Duke University, and his M.Eng. in biomedical engineering at Cornell University. His research focus is on melding 3D printing and microfluidics technologies in the pursuit of vascular tissue engineering.

Wei Zhu is a postdoctoral fellow at the University of California, San Diego in the Department of NanoEngineering working under Dr. Shaochen Chen. He received his B.S. (2012) in optical engineering at Zhejiang University, and his M.S. (2014) and Ph.D. (2016) in nanoengineering from UC San Diego with an emphasis on biomedical nanotechnology. His research focuses on the development of advanced 3D bioprinters and 3D printing of functional biomaterials for tissue modeling.

Shaochen Chen is a Professor in the NanoEngineering Department at the University of California, San Diego. He is a founding codirector of the Biomaterials and Tissue Engineering Center. He had been a Professor at the University of Texas at Austin and Nanomanufacturing Program Director at the National Science Foundation. His research interests include 3D bioprinting, biomaterials and nanomaterials, tissue engineering, organ-on-a-chip, and nanomanufacturing.

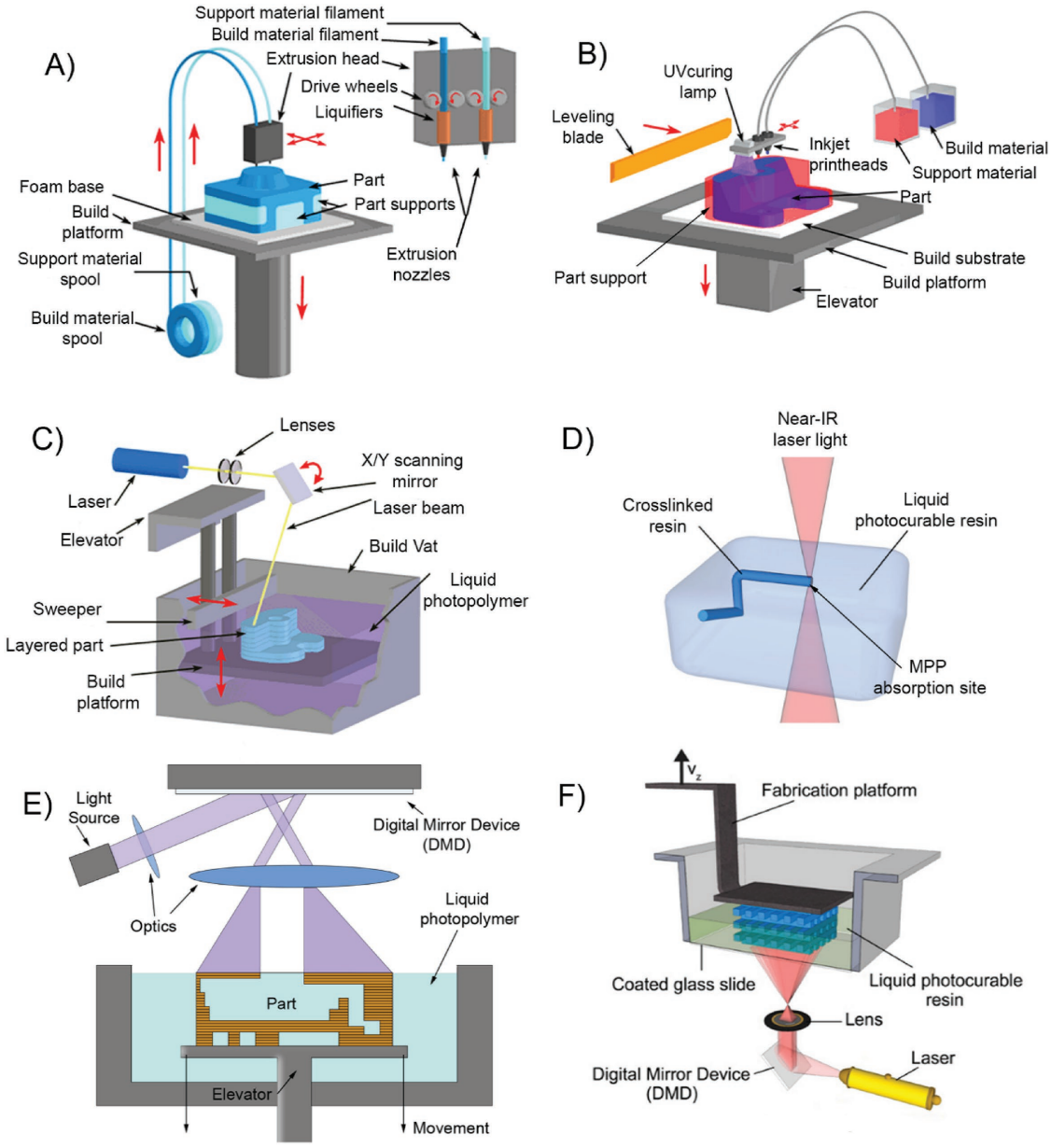

Figure 1. Schematic overview of various E-3DP and L-3DP modalities. A) E-3DP: Schematic of an FDM 3D-printer, where thermoplastic filaments spool through a heated nozzle extruder. B) E-3DP: Schematic of an MJM 3D-printer, where materials are jetted via printheads. The variant pictured photopolymerizes the dispensed droplets in place. C) L-3DP: Schematic of a traditional SLA 3D-printer, where a laser beam is raster-scanned across the surface of a photopolymerizable resin as a build stage within moves. A–C) Adapted with permission.[5] Copyright 2016, The Royal Society of Chemistry. D) L-3DP: Multiphoton polymerization 3D-printing, where nonlinear photon absorption from a laser into a photopolymerizable resin creates structures as the laser is traced in 3D space. E) L-3DP: The "free surface" configuration digital-light-processing 3D-printing, where a 2D cross-section of light strikes the air–liquid surface of a photopolymerizable resin as a build stage sinks into the vat. F) L-3DP: The "bat" configuration of digital-light-processing 3D-printing, where a 2D cross-section of light strikes the bottom of a transparent vat of photopolymerizable resin, as a build stage pulls out of the vat. D,F) Adapted with permission.[6] Copyright 2012, Elsevier.

are dispensed in a layer-by-layer fashion via numerous nozzles contained in movable printheads. The difference with MJM as compared to commercial inkjet printers is that these droplets are commonly composed of a liquid prepolymer, which are then crosslinked quickly after deposition (either through thermal cooling or photopolymerization) such that each layer is bonded to the previously deposited layer, thus building the final 3D object. The multiple-nozzle approach to the printhead means that an MJM printer can deploy multiple materials simultaneously in a single pass. Some MJM printers can also deliver gel or wax-like sacrificial materials, which, after postprocessing removal, allows the construction of 3D-objects with void spaces, in addition to multiple materials (and thus multiple material properties) in any given layer.

2.2. Light-Based 3D-Printing

L-3DP fundamentally uses light as the primary effector for fabrication—historically, this category was filled mostly by SLA, where ultraviolet laser light was raster-scanned across the surface of photopolymerizable resins. In the last two decades, since Hull first coined the term "Stereolithography" in 1986,[9] however, L-3DP has come to encompass a wide variety of materials, light sources, and motion control. Material choices can include the gas, liquid, and solid phases of matter; light sources can range from the deep UV all the way to the upper end of the visible spectra, and the light itself can be controlled to strike not just surfaces but also within the depths of a photopolymerizable material.[10] In this context of fabricating functional biomedical microdevices, most L-3DP technologies still rely on the photopolymerization of liquid prepolymer into solid, cured entities.

By "photopolymerization," we refer to the set of light-induced polymerization reactions in which the energetic absorption of light by a photosensitive material causes chain-growth crosslinking and polymerization of functional monomers into polymers.[11] Whether the material is directly photopolymerized or mediated by photo-crosslinking agents can depend on user needs, but most L-3DP systems commonly utilize free-radical polymerization (FRP). The FRP process is briefly described as follows: (i) light strikes a photoinitiator molecule that then generates free-radical species; (ii) these free-radical species interact with functional monomers; (iii) these active monomers then react with other monomers in a propagative manner to produce polymeric chains until reaction termination. After the photopolymerization and motion-related steps in the 3D-printing process are completed, any unreacted materials can be easily flushed away to yield the final 3D object. Since photopolymerizable materials only change their properties (namely a phase transition from liquid to solid) upon exposure to light, advances in light-3DP technologies have enabled quick fabrication of high-resolution functional microdevices.

2.2.1. Direct Laser Writing

Direct laser writing (DLW) is a type of L-3DP where focused laser light is used to illuminate a single focal point, either on the surface or within a volume of photopolymerizable materials; digitally controlled motorized stages and/or mirror galvanometers can then trace this illuminated focal point in 3D space to fabricate a 3D structure. Common examples of DLW technology include SLA and multiphoton polymerization (MPP). SLA is a single-photon polymerization process in which the laser light source is raster-scanned across the surface of a liquid prepolymer, after which the focal plane is changed such that a new layer can be irradiated and adjoined in a layer-by-layer fashion to build the final 3D object. For this reason, SLA printers operate in what is called a "free-surface configuration," termed for how the light strikes the photopolymerizable resin at the air–liquid interface. The SLA's resolution limit depends mostly on the photopolymerizable material's absorption spectra, the laser's focal point size, and the precision of the motorized stage.

In contrast, MPP operates not by projecting light onto a 2D surface, but rather into a 3D voxel within the depths of a photopolymerizable material. MPP materials undergo polymerization after the nonlinear absorption of two or more photons (in contrast to the ones used in SLA, where a single photon is sufficient): to aid in this, MPP systems typically use high-intensity pulsed lasers with a very short pulse duration, i.e., femtosecond pulsing. Only the material at the laser's focal point undergoes polymerization due to the multiphoton absorption, since the intervening regions are effectively transparent to the wavelength used and do not receive enough energy to catalyze polymerization. Tracing the laser's focal point in 3D space then enables free-form fabrication of 3D structures, and MPP's precision enables the creation of sub-micrometer features in the regime of 100 nm in size.

2.2.2. Selective Laser Sintering/Melting

Selective laser sintering and selective laser melting (collectively known as powder-bed fusion techniques, but labeled here as SLS/M) are loosely related to direct laser writing in that a high-powered laser light is used to selectively sinter or melt, respectively, powdered materials into 3D structures. This is contrasted against photoinitiated chemical methods as seen in SLA or MPP 3D-printing, as SLS/M techniques utilize the energy of the laser to thermally heat the powdered building substrates until they physically fuse together. In most SLS/M setups, the laser light scans across the build substrate one layer at a time, after which fresh powdered material is mechanically laid across as the next layer, ready to be fused to its predecessor. The resolution of SLS/M techniques depends on the laser power, scanning speed, and materials used, but often the final products are characterized on the basis of porosity—both pore density and pore size.[12] SLS/M is mentioned here for conceptual similarity to DLW, but as the majority of SLS/M materials are neither biocompatible nor biodegradable,[13] beyond applications to certain tissue-engineered scaffolds,[12] which are outside the scope here, fabrication of functional biomedical microdevices via this method is limited.

2.2.3. Digital Light Projection

Digital light projection (DLP) 3D-printing, termed here as DLP-3DP, is a variant of "standard" SLA where, instead of a raster-scanned laser, a spatial light modulating (SLM) element, such as a liquid-crystal display (LCD) or digital micromirror device (DMD), is used as a dynamically changing "digital photomask" in projecting a 2D plane of specifically patterned light.[14] By directing this light plane onto a vat of photosensitive substrate, DLP-3DP allows the photopolymerization of an entire 2D cross-section in a single exposure, subsequently enabling the fabrication of 3D constructs simply by changing the vertical position of the focal plane and selectively curing adjacent layers together. Similar to DLW-based techniques, the resolution limits for DLP-3DP are dependent mostly on the material's photopolymerization properties, the motorized stage's precision-of-movement, and the size of the projected "pixel." Two main configurations

of DLP-3DP exist, termed: (i) "free surface," where photopolymerization happens at the air–liquid interface and the build stage moves "downward" into the build vat of material, and (ii) "bat" or "upside-down," where the light plane is directed at the bottom surface of a transparent build vat and the build stage rises upward from the floor, thus "pulling" the 3D object from the fluid as it prints.

Integral to DLP-3DP is the SLM element, which circumvents the need for physical photomasks by providing a digitally controlled, two-dimensionally projectable image. There are two main options for the SLM element: LCD or DMD, both of which can spatially modulate incoming light to produce an outgoing pattern. To briefly describe their modes of function: LCDs contain layers of liquid crystals and electrodes sandwiched between polarizing filters—incoming light is modulated by applying electrical current to the electrodes in desired areas, causing the liquid crystals there to align such that light cannot pass through. DMDs are opto/electromechanical arrays of micromirrors on individually addressable tilt switches, where each micromirror has an "on" or "off" state that allows selective reflection of incoming light—toggling individual mirrors in desired areas thus creates the desired images.

The use of LCDs as a DLP-3DP method was initially popularized by Bertsch et al. in 1997.[15] The LCD spatially modulated an expanded laser beam, where the transmitted light was focused and directed to strike the surface of a motorized stage submerged in photopolymerizable resin. DMDs were originally manufactured by Texas Instruments in 1987. While they enjoyed commercial success in digital entertainment systems, their utilization in DLP-3DP methods happened later, with early examples utilizing visible and UV light demonstrated by Bertsch et al.[16] and Beluze et al.[17] in 1999. They utilized DMD chips with video graphics array (VGA) resolution (640 × 480) in conjunction with broadband metal halide lamps, with desired wavelengths obtained by selective optical filtration. As understanding of DMD technology improved in sophistication and resolution, so too did DMD-based 3D-printing: Sun et al. in 2005 demonstrated high-aspect-ratio structures, some with features as fine as 0.6 μm,[18] and Lu et al. in 2006 showed the earliest known example of direct DMD-projection printing of biocompatible materials into 3D scaffolds for tissue engineering.[14] More recently, Tumbleston et al. demonstrated "continuous liquid interface production (CLIP)," where, in the "bat" configuration of DLP-3DP, they utilized an oxygen-permeable membrane to inhibit polymerization where a DLP is used to project a 2D light plane up into a vat of photopolymerizable resin—they demonstrated the use of an oxygen-permeable membrane at the light's focal plane, such that prints-in-progress did not "stick" to the build-vat floor, increasing the speed at which the 3D-printing could occur.[19]

3. 3D-Printing of Functional Biomedical Microdevices

The variety of 3D-printing methodologies has enabled the creation of a wide array of functional biomedical microdevices, encompassing different form factors and capabilities. In this section, we go over the use of different 3D-printing techniques for various biomedical microdevices, including micromachines, personalized medicines, biosensors, and microfluidic devices.

3.1. Micromachines and Robotics

Microscale machines and robotics are often challenging to produce due to their small size, which scales with the complexity of the final device—mechanical features and forces that may be well understood at the macroscale may function differently at the microscale, necessitating material and/or design changes. As an example, we consider the problem of microscale propulsion: many microorganisms exist in fluid environments where viscous forces dominate inertial forces, otherwise known as the low Reynolds' number regime. In such environments, traditional mechanical elements for locomotion, i.e., gears, motors, and shutters, are less effective due to enhanced friction at the microscale. Thus, when designing for locomotion in low Reynolds' number regimes, often special design considerations must be taken into account, most notably Purcell's scallop theorem, which states that locomotion in fluids of low Reynolds' number regimes must generally be of nonreciprocal and time-asymmetric character.[20]

3D-printing has enabled innovative ways of actualizing microscale locomotion—Tottori et al., inspired by bacterial flagella, reported the fabrication of magnetically controllable helical micromachines that could swim in both water and fetal bovine serum[21] (**Figure 2**a). A two-photon polymerization (2PP)-based 3D DLW was used to fabricate helical structures in a photoresist, followed by physical vapor deposition of magnetically sensitive Ni/Ti bilayers; externally applied rotating magnetic fields induced rotational motion in the helices, and thus propulsion. The flexibility of their 3D DLW system enabled iteration of their helical micromachines through various design parameters, such as length, diameter, and helical angle, with sub-micrometer resolution. For added utility, cage-like microholders were added to one end of the helices to allow the manipulation and transportation of microparticle cargo, opening up potential applications of such micromachines in manipulation of biological samples, or targeted drug delivery at the microscale.

Purcell's scallop theorem holds generally for locomotion in Newtonian fluids, but in non-Newtonian fluids with shear-thickening or shear-thinning properties, i.e., hyaluronic acid, blood, and saliva, the theorem no longer holds and low Reynolds' number propulsion can be realized with reciprocal motion.[22] Qiu et al. reported microswimmers with scallop-like shapes that could perform reciprocal opening/closing body-shape changes, and swim in non-Newtonian fluids. To fabricate these "micro-scallops," an MJM 3D-printer was used to create a negative mold out of a rigid thermoplastic material, which was subsequently cast with poly(dimethylsiloxane) (PDMS) and outfitted with two micromagnets on the "shells" (Figure 2b). By magnetically introducing a time-asymmetric stroke pattern in the opening/closing of the shells, and by exploiting the strain-rate-dependent viscosity of the non-Newtonian fluids, Qiu et al. demonstrated the propulsion of their microscallops in both shear-thickening (fumed silica in poly(propylene glycol)) and shear-thinning (hyaluronic acid) solutions.[22]

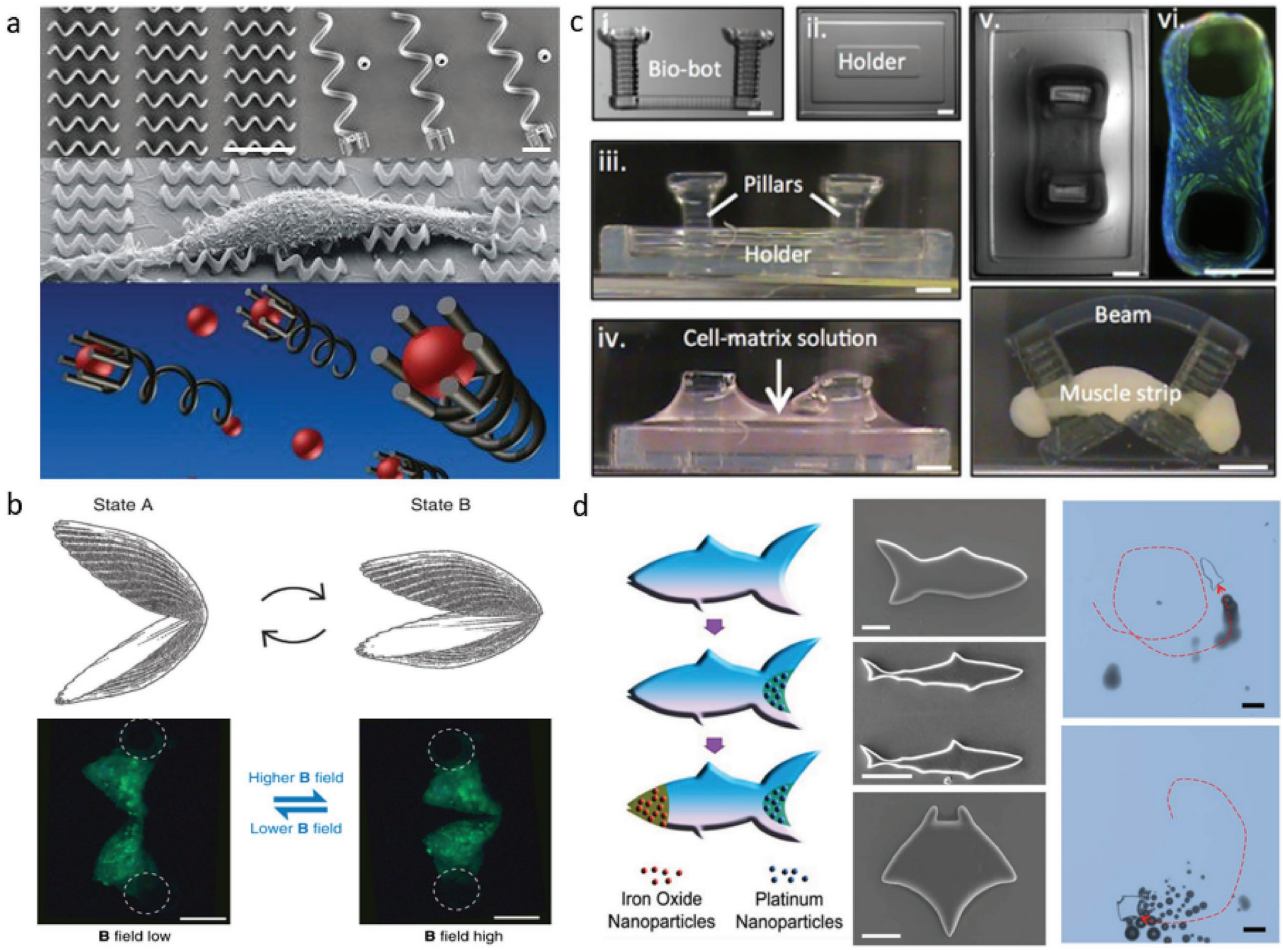

Figure 2. 3D-printing of micromachines and microrobotics. a) Magnetic helical micromachines fabricated by 2PP-based 3D-DLW. Scale bar: 10 µm. Adapted with permission.[21] Copyright 2012, Wiley-VCH. b) Magnetic microscallops capable of locomotion in non-Newtonian fluids, fabricated by MJM and PDMS microcasting. Scale bar: 200 µm. Adapted under the terms of the Creative Commons Attribution 4.0 License.[22] Copyright 2014, Macmillan Publishers Limited. c) A hydrogel "bio-bot" powered by the actuation of skeletal muscle strips, fabricated by SLA 3D-printing. Scale bar: 1 mm. Adapted with permission.[23] Copyright 2014, The National Academy of Sciences. d) 3D-printed hydrogel microfish with diverse biomimetic structures and controllable locomotive capabilities. Scale bar: 50 µm. Adapted with permission.[24] Copyright 2015, Wiley-VCH.

In addition to magnetic materials, biological components such as cells and/or tissues can be incorporated into soft robotics to provide the propulsive forces. Cvetkovic et al. developed a 3D-printed hydrogel "bio-bot" powered by the actuation of skeletal muscle strips (Figure 2c).[23] An SLA 3D-printer was used to fabricate the millimeter-scale bio-bots out of poly(ethylene glycol) diacrylate (PEGDA) hydrogel. Their bio-bots featured two stiff pillars connected by a compliant beam, around which skeletal muscle myoblasts and extracellular matrix proteins were polymerized into strips. An externally applied electrical field induced contraction in these muscle strips, in turn causing contraction in the bio-bot's pillars, ultimately mimicking an inchworm-like "crawling" movement. Cvetkovic et al.'s SLA 3D-printer's flexible control over laser energy dosage enabled fabrication of bio-bots with tunable mechanical properties and structural conformations, allowing the testing of bio-bots with both symmetric and asymmetric pillar lengths, of which they found that asymmetric pillar designs afforded better controlled directional movement.

Besides biologics, additional utility can be gained by incorporating other components, such as functional nanoparticles—Zhu et al. reported 3D-printed biomimetic "microfish" with nanoparticle-granted locomotion and detoxification capabilities (Figure 2d).[24] A DLP-3DP printer—a DMD-based microscale continuous optical printing system (μCOP)—directly printed the microfish, utilizing a photopolymerizable PEGDA-based hydrogel as the matrix material, additionally encapsulating functional nanoparticles. With the μCOP system's high resolution, Zhu et al. were able to print magnetic iron oxide (Fe_3O_4) nanoparticles and platinum (Pt) nanoparticles into the head and tail of the microfish, respectively, thus providing magnetically controllable chemical propulsion in the presence of hydrogen peroxide as a fuel. As a proof of concept, they incorporated toxin-neutralizing polydiacetylene nanoparticles, granting detection and detoxification capabilities against the pore-forming toxin melittin. They further demonstrated that the mobile microfish exhibited higher detoxification efficiency compared to stationary ones, and that the flexibility

of their μCOP system enables the fabrication of freely swimming microfish of various shapes and functional nanoparticle loadouts.

3.2. Pharmaceuticals and Drug Delivery

In the previous section, we discussed the development of micromachines and robotics using different types of 3D-printing technologies. One potential application of such 3D-printed microdevices lies in the domain of customized medicines and targeted drug delivery, where numerous efforts to explore the feasibility of 3D-printed approaches have been made.[25–31] Here, building off previous reviews in the field,[32–35] we focus on recent examples of utilizing 3D-printing specifically for pharmaceutical manufacturing and drug delivery.

With pharmaceutical and biological compounds meant for human use, approval by the U.S. Food and Drug Administration (FDA) and similar institutions is a long and arduous process—the drugs themselves, as well as any excipients, solvents, and/or other process steps must be exhaustively tested. Inkjet-based and, more recently, extrusion-based 3D-printing technologies have come to the forefront of 3D-printing in pharmaceutical manufacturing, as with little-to-no mechanical modification they are well-suited to manipulating drug–excipient formulations, i.e., powder blends, aqueous binding, pastes, etc.[33] Scoutaris et al. explored the feasibility of using a modified inkjet printer to produce a 2D-array of microspot formulations for controlled drug release (**Figure 3**a)[26]—felodipine, an antihypertensive drug, was dispersed in the excipient (poly(vinylpirrolidone), and deposited as droplets with diameters of less than 100 μm. The stable dispersion and intermolecular level interaction between the drug and the excipient were confirmed by atomic force microscopy and attenuated-total-internal-reflection infrared spectroscopy. It was also found that the drug-release profile can be controlled by the drug-loading ratio, indicating the potential of using 3D-printing to tailor practical dosage forms to the individual needs of specific patients.

One limitation with the 2D microdroplet deposition employed by Scoutaris et al. is that due to the 2D nature of the printed products, there is an upper limit to the amount of drug that can be loaded into the microdroplets. Khaled et al. addressed this limitation in their work, employing a nozzle-based extrusion 3D-printer to fabricate larger form-factor guaifenesin bilayer tablets (GBT) (Figure 3b).[31] Their 3D-printed GBTs feature similar dimensions to their commercial counterparts, and their formulations were adjusted such that they had comparable drug-release profiles as well. By tuning the chemical composition of the drug and associated excipients, Khaled et al. were able to bring various physical and mechanical properties, such as weight uniformity, hardness, and friability into compliance with international standards set by the United States Pharmacopeia. The printing process in this study was achieved via a low-cost desktop 3D-printer operating at room temperature, underscoring the potential of using such techniques for printing personalized, point-of-care medicine in decentralized facilities, such as the patients' own homes.

Nozzle-based extrusion 3D-printers are flexible in both construction and utility, such that adding multiple nozzles enables multimaterial 3D-printing, with each nozzle capable of extruding a different type of filament. Goyanes et al. employed such a setup to fabricate multidrug caplets with two different types of internal structure—multilayer, and core–shell configurations (Figure 3c).[30] Paracetamol and caffeine were selected as the model drugs due to their prevalence in combinational use in commercial medicines. In the multilayer configuration, caffeine and paracetamol layers were deposited in an alternating fashion, while in the core–shell configuration, they were the core and shell, respectively. Raman spectroscopy mapping was used to confirm the localization and separation of the two drugs in their respective compartments. Interestingly, unique drug-release profiles were found for these two configurations due to their different internal structures. The multiplayer configuration showed a simultaneous release of the two drugs loaded in the adjacent layers, while with the core–shell configuration, delayed release of the drug loaded to the core compartment was achieved, and the lag-time can be modulated by the shell layer. This study highlighted the advantages of 3D-printing over conventional drug manufacturing methods to fabricate devices loaded with multiple medicines and customize unique drug-release profiles with specialized design configurations.

As another example of the viability and suitability of 3D-printing techniques for complex medication regimes, Khaled et al. demonstrated extrusion-based 3D-printing of a "polypill," a construct with five compartmentalized drugs, with two independently controlled and well-defined release profiles, intended as a comprehensive cardiovascular treatment regime.[29] The polypill was formulated and printed such that there was an immediate release compartment of aspirin and hydrochlorothiazide, and three sustained release compartments of pravastatin, atenolol, and Ramipril, respectively (Figure 3d). To prevent unwanted interaction between the five different drugs, a hydrophobic cellulose acetate shell with controlled porosity was printed first; then, the separate drugs were extruded into their respective compartments. In addition to verifying immediate and sustained release profiles for their chosen drugs, X-ray powder diffraction (XRPD) and Fourier transform infrared (FTIR) spectroscopy data showed that there were no detectable interactions between the drugs and the polypill's excipients, as well as no detectable changes in the drugs' structural forms. Their 3D-printed "polypill" concept represents not only improved on-demand personalization of drug combinations and release profiles but also a potential way to improve patient compliance with multidrug and variable dosing regimens at the point of care. Indeed, the FDA recently approved the first 3D-printed pill for the drug levetiracetam in 2015, under the tradename Spritam[36] underscoring the progress that 3D-printing has made in the pharmaceutical domain.

Light-based 3D-printing methods, such as DLW or SLA, have seen limited success on the pharmaceutical manufacturing front, likely due to the arduousness of approving photopolymerizable resins for human drug usage, in addition to the potential degradation complications of using UV and/or visible light during the printing process.[33] That said, instances of using light-based 3D-printing as an approach for producing drug-delivery methods have been reported, mostly in the form of microneedles as medical devices—a salient example being that of the successful delivery of an influenza vaccine utilizing microneedle arrays.[37] Conceptually, microneedles are

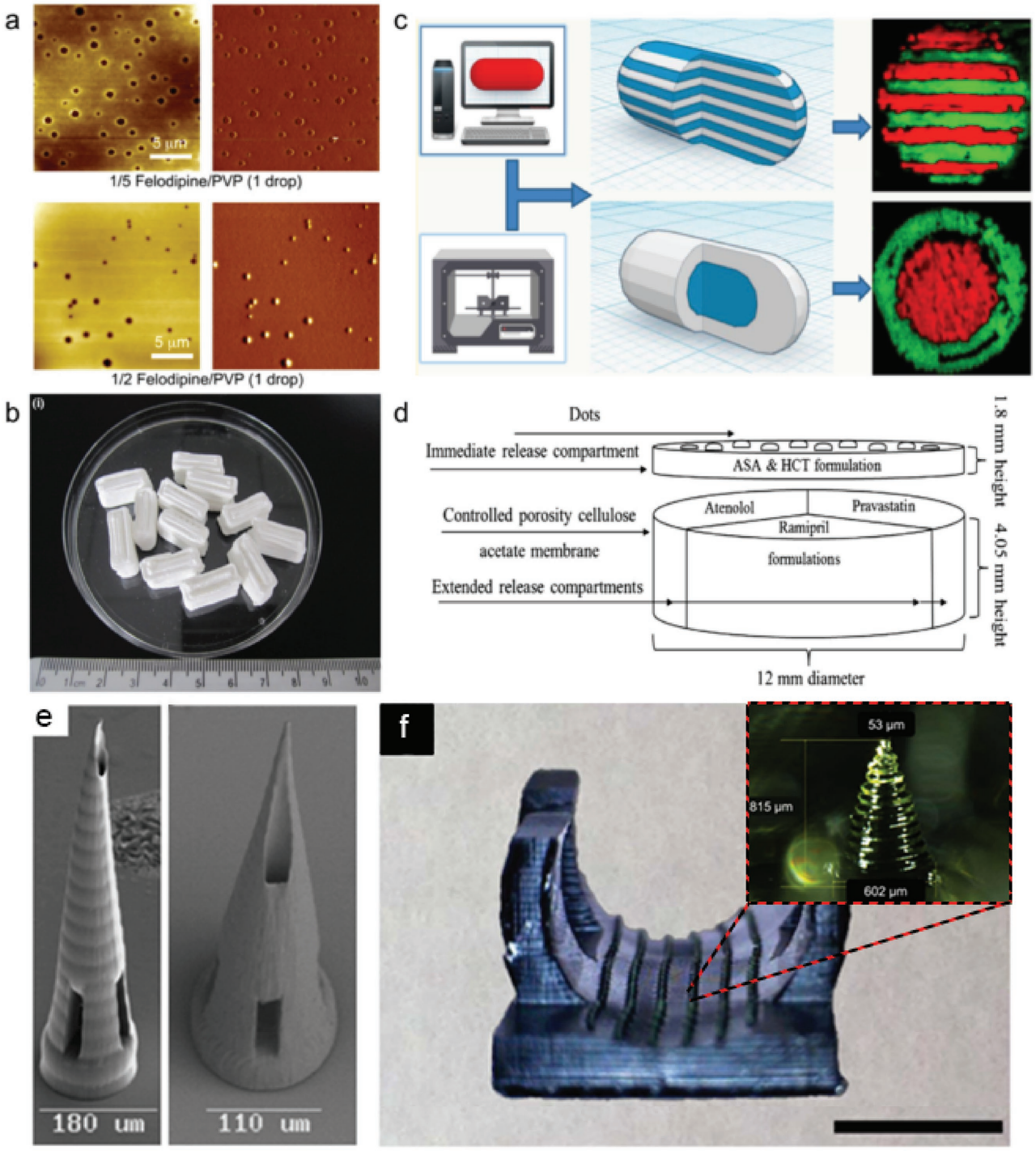

Figure 3. 3D-printing of medicines and drug delivery vehicles. a) 2D array of microspot formulations for controlled drug release, fabricated by an inkjet printer. Adapted with permission.[26] Copyright 2011, Elsevier. b) 3D-printed guaifenesin bilayer tablets with sustained drug-release profile, fabricated by an extrusion-based printer. Adapted with permission.[31] Copyright 2014, Elsevier. c) Multidrug caplets with two different internal structures—multilayer and core–shell, printed by a multinozzle 3D-printer. Adapted with permission.[30] Copyright 2015, American Chemical Society. d) Schematic structural diagram of the 5-compartment polypill design. Adapted with permission.[29] Copyright 2015, Elsevier. e) SEM image of MPP-3DP-generated microneedles, fabricated from a commercially available polymer–ceramic hybrid material. Scale bars: 180 μm (left), 110 μm (right). Adapted with permission.[43] Copyright 2007, The American Ceramic Society. f) DLP-3DP-generated microneedles printed as part of a personalized contoured surface meant for splinting a finger with trigger finger disorder. Scale bar: 2 cm. The inset shows a closeup view of one microneedle, sized 815 μm tall, 602 μm diameter base, and 53 μm diameter tip. Adapted with permission.[45] Copyright 2017, Institute of Physics.

miniaturized versions of the standard clinical hypodermic needle, but, due to advances in microfabrication technology, they can be made to have more therapeutic utility: arrays of hollow microneedles can deliver or receive a broad range of compounds in clinically useful amounts, while also avoiding some of the pitfalls of hypodermic needles, i.e., mishandling due to lack of training,[38] or limited patient compliance due to pain[39] and "needle-phobia."[40] More details and numerous examples of microneedle fabrication, function, and application can be found in other microneedle-specific reviews,[38,41,42] but the next few examples focus on microneedles that have been fabricated by light-based 3D-printing. Ovsianikov et al. used 2PP-3DP to fabricate hollow microneedles out of an organically modified ceramic material in an effort to impart durability during insertion into the skin, as microneedle breakage could be detrimental to the therapeutic delivery process. Their microneedles were 800 μm long, with bases ranging from 150 to 300 μm, and were successfully tested on cadaveric porcine adipose tissue without microneedle fracturing[43] (see Figure 3e for a scanning electron microscopy (SEM) image of representative microneedles). Kochhar et al. utilized SLA-based 3D-printing to photopolymerize PEGDA hydrogels into microneedles containing bovine serum albumin (BSA) as a stand-in model drug;[44] these microneedles averaged 820 and 300 μm in length and diameter, respectively. Their microneedles were found to be stable, of low cytotoxicity to human cells across three different cell lines, and, most importantly, enhanced BSA delivery through rat skin compared to passive diffusion, thus demonstrating their utility in transdermal therapeutic delivery. Lim et al. were able to successfully utilize DLP-3DP in printing microneedles onto a contoured surface, in contrast to most other fabrication methods that are limited mostly to planar surfaces (see Figure 3f to see the microneedle-laden contour). In a departure from the concept of having microneedles with drug reservoirs, Lim et al.'s microneedle array only penetrated the skin to provide enhanced absorption of topically applied drugs, in this case a commercially available topical diclofenac diethylamine 1.16% gel for pain associated with finger-joint inflammation.[45] Their microneedles were 800 μm tall, with base and tip diameters of 600 and 50 μm, respectively, and five-fold enhanced delivery of topical diclofenac via microneedles by 1.5 h compared to intact skin permeation alone was able to be demonstrated. While Lim et al.'s microneedles were susceptible to fracturing at the tips, biocompatibility testing of their material deemed that any tips that might be left behind in the skin were non-irritative, an important consideration when dealing with numerous, fragile microneedles. Such examples showcase the potential for such microneedles to serve as an alternative to traditional hypodermic needle injection, and represent the continued advancement of a new paradigm in painless, versatile transdermal therapeutic delivery.

3.3. Biosensors

Biosensors are a class of devices that interface biological analytes of interest with electrical, physical, and/or chemical transducers—they can "sense" the presence and/or amount of an analytical target, and thus are of significant interest to many industries, e.g., military, food science, and medicine.[46] The advance of the semiconductor industry in recent decades has created a robust variety of sensing technologies, but 3D-printers have found success in fabricating low-cost, custom-built objects that can not only function as a supportive infrastructure for existing sensor technologies but also in making biosensing devices from the ground up. Building from previous reviews in the field of 3D-printed biosensing technology,[4,47,48] here, we explore examples of 3D-printed biosensing platforms, ranging from assemblies of custom and commercial pieces to wholesale construction of new devices.

One class of technology significant to the biosensing domain is point-of-care devices—these devices are usually simple in construction, easy to operate, and portable, for decentralized use out in the field or on-demand. Assembling custom 3D-printed pieces with commercially available technologies can enhance the properties of existing sensor technologies, such as allowing the interfacing of disparate components and increasing portability—an example of such comes from Gowers et al., who utilized both DLP-3DP and MJM-3DP systems to fabricate microfluidic devices and electrode holders to not only pair with each other but also integrate with clinically available microdialysis probes for real-time monitoring of metabolic activity.[49] They were able to demonstrate their setup in reporting the glucose and lactate levels of cyclists during exercise, while the monitoring devices were attached to the cyclists themselves. Boehm et al. fabricated a microneedle-based fluid-sampling system for assessing histamine contamination in tuna[50]—DLP-3DP was used to fabricate an array of fluid-capturing microneedles and a custom lateral flow chamber, where commercially available histamine-detecting test-strip assays could be placed. Their microneedle arrays were stabbed into histamine-contaminated tuna for 5 s, where the fluid retained in the microneedles could then be flushed into their lateral flow chamber for detection via the test strips. While Boehm et al. observed a discrepancy between their custom system and the commercial kit at low histamine levels, improved statistical agreement was found between the procedures at higher histamine levels, which shows promise when combined with the fact that their microneedle-based assay utilized 1/7th of the volume of reagents and significantly less sample preparation, as compared to the commercial kit's standard procedure.

Roda et al. combined a consumer-grade smartphone with parts fabricated via a low-cost FDM 3D-printing system to make a point-of-care biosensor package for measuring L-lactate levels in bodily fluids. A disposable 42 × 28 mm reaction analysis chamber was designed and fabricated such that it could attach to the smartphone, where its camera could measure the light produced by a luminol/H_2O_2/HRP CL enzymatic reaction carried out inside the attachment's body.[51] Their group was able to demonstrate real-time monitoring of lactate levels in human sweat during exercise. Similarly, Cevenini et al. utilized FDM to print smartphone-paired assay reaction chambers, reporting a cell-based toxicity biosensor utilizing the smartphone's camera to analyze toxicity-induced bioluminescence in genetically engineered cells (**Figure 4**a).[52] To improve assay longevity, they immobilized their chosen cells (human embryonic kidney cells transfected to produce luciferase) in agarose, and to provide ease-of-use, they custom-coded their own smartphone

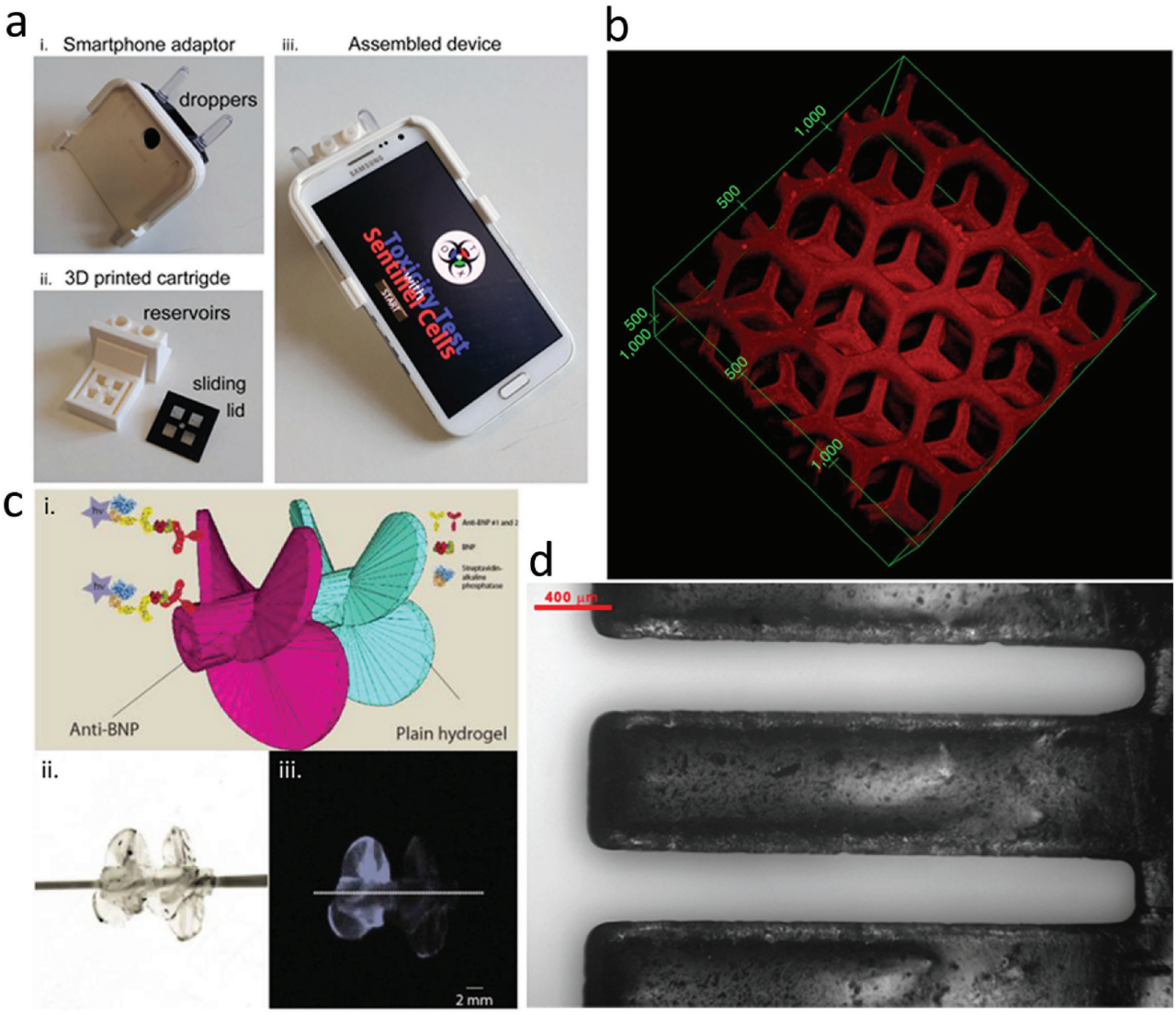

Figure 4. 3D-printing of biosensors. a) Smartphone-coupled cell-based toxicity reaction ware, printed via FDM-3DP. Adapted with permission.[52] Copyright 2016, Elsevier. b) Dual-purpose toxin sensor and detoxification device based on liver microarchitecture, fabricated via DLP-3DP. Units shown: µm. Adapted with permission.[55] Copyright 2014, Nature Publishing Group. c) Impeller biosensor with antibodies incorporated into body fabricated via DLP-3DP; sensing efficiency increases when spun. Scale bar: 2 mm. Adapted with permission.[56] Copyright 2016, American Chemical Society. d) Mass-sensing cantilevers with incorporated functional groups, fabricated via DLP-3DP. Scale bar: 400 µm. Adapted with permission.[57] Copyright 2017, American Chemical Society.

application; their results were found to be comparable to commercial assays and centralized laboratory testing. These examples showcase the potential of portable, point-of-care analysis that results from interfacing already-existing technology with simple, low-cost 3D-printed plastics.

Beyond fabricating a supporting infrastructure for existing sensor technology, 3D-printing also makes it possible to directly integrate sensing capabilities into the structures of printed constructs, thus more closely linking form and function. Miller et al. reported an electrochemical transducer platform consisting of DLP-3DP-fabricated hollow-microneedle arrays,[53] where the triangularly sloped microneedles bore chemically modified carbon-fiber electrodes. These electrode–microneedle constructs were shown to be able to detect hydrogen peroxide and ascorbic acid, but, in principle, they can be used to detect any analyte of interest so long as there is a corresponding chemical modification available for the electrodes used.

Kim et al. utilized DLP-3DP to directly photopolymerize polymer composites impregnated with piezoelectric nanoparticles into 3D microstructures, demonstrating free-form construction of piezoelectric polymers into arbitrary geometries.[54] As piezoelectric substances are capable of converting mechanical forces into an electric charge and vice versa, they show high potential for use in biosensing applications where traditional ceramic piezoelectric materials would be unsuitable. Gou et al. reported a biomimetically derived biosensor, utilizing DLP-3DP to fabricate a hybrid sensing/detoxification device—hydrogel composites were impregnated polydiacetylene nanoparticles

and optically printed into 3D-microarchitectures resembling the hexagonally based native architectures of liver lobules (Figure 4b).[55] Their bioinspired detoxification device demonstrated high efficacy in sensing, attracting, and neutralizing harmful pore-forming toxins.

In addition to static sensors, other groups have demonstrated sensors that can move and actuate to increase their functionality in addition to biosensing capability. Mandon et al. demonstrated the use of DLP-3DP to fabricate antibody-laden hydrogels into 3D structures capable of directly interacting with their environment to enhance sensing sensitivity—one of their trials described a 3D-printed propeller composed of a PEGDA hydrogel loaded with anti-brain natriuretic peptide (anti-BNP) monoclonal antibodies (Figure 4c); rotating the propeller at 150 rpm in BNP solution increased the magnitude of chemiluminescent signaling fivefold compared to when it was not rotating at all.[56] Stassi et al. utilized DLP-3DP to fabricate bisphenol-A ethoxylate diacrylate into microcantilevers for mass-sensing applications—these polymeric microcantilevers incorporated acrylic acid into the prepolymer solution to impart biomolecular functionalization capability to the surfaces of the cantilevers (Figure 4d).[57] Their one-step fabrication, combined with the intrinsic surface functionalization provided by the acrylic acid, was contrasted against traditional microfabrication processes for making silicon biosensing cantilevers. Stassi et al.'s microcantilevers were implemented in a gravimetric assay utilizing recombinant protein G and horseradish-peroxidase-conjugated goat anti-mouse immunoglobulin G, where they found that the presence of biomolecules on the cantilevers resulted in tangible shift of more than 20 times the cantilevers' mean relative resonant frequencies. Such devices demonstrate the potential for easily fabricated, "intrinsically functional" biosensors across a variety of sensing applications, and show promise in advance 3D-printed biosensing platforms.

3.4. Microfluidics

Microfluidic systems comprise the foundational basis for "micro total analysis" systems, or "lab-on-a-chip" devices, where microscale architectures can be used to precisely control small quantities of reagents and/or analytes of interest. Traditional methods of manufacturing microfluidic systems are still largely rooted in cleanroom-based 2D photolithography and PDMS microcasting,[58–60] but 3D-printing has gained prominence due to its design flexibility, rapid prototyping, and on-demand production capability. With an additive manufacturing approach, greater liberties can be taken in the construction of the final microfluidic device, with the possibility of creating architectures that may be challenging to produce using traditional methods—examples range from simply decreasing production time between design and fabrication (compared to photolithography/microcasting), the creation of challenging features such as high-aspect-ratio 3D geometries for PDMS micromolding, or directly printing devices with isolated microchannels and void spaces.

Microfluidic devices crucially depend on precisely formed void spaces through which fluids, reagents, or other materials flow, and 3D-printers must take into account many different parameters to ensure success; examples include microchannel dimensions, interior surface smoothness, and sealable/perfusable interiors. Various groups have approached the problem of 3D-printing-viable microfluidic devices, with differing levels of utility, complexity, and success—we review these bodies of work, building upon previous review articles in the field of 3D-printed microfluidics.[5,61,62]

Morgan et al. recently reported using an off-the-shelf FDM-3DP to create flow-focusing junctions with channel dimensions as small as 400 μm, with the device itself exhibiting properties crucial to microfluidics, such as optical transparency and high structural strength (leak-free up to 2000 kPa).[63] Bishop et al. utilized a commercial FDM-3DP to fabricate microfluidic devices geared toward Prussian Blue nanoparticle preparation and electrochemically based hydrogen peroxide sensing, each with sealed, perfusable channels of 800 μm × 800 μm square dimensions.[64] Commercial entity Dolomite produces an off-the-shelf desktop FDM-3DP system for direct fabrication of sealed, perfusable microfluidic devices out of cyclic olefin copolymer at a resolution limit of 320 μm (width) by 125 μm (height), and sells devices geared toward any number of biomedical applications, ranging from biomedical assays and diagnostics to chemical synthesis and drug development.[65]

There are few examples of microfluidic devices made via MJM-3DP systems, in part due to the difficulty in removing the sacrificial materials utilized to fill the void spaces made during printing,[66] but functional biomedical microdevices have nonetheless been reported. Erkal et al. utilized a commercially available MJM 3D-printer to fabricate simple straight-channel microfluidic platforms that housed electrochemical electrodes.[67] Their featured electrodes were made of either glassy carbon or platinum black (for the detection of dopamine or nitric oxide, respectively), but the modular nature of their design allows the possibility of multiplexing any potential number of electrochemical electrode setups. Begolo et al. utilized MJM-3DP to produce multimaterial "pumping lids" that could be placed over the inlet(s) of other microfluidic devices so as to provide equipment-free pressure and/or vacuum influence.[68] Causier et al. MJM-3D-printed a 4-piece "bubble pump" for use as an NMR imaging cell, and had a self-contained fluidic system composed of a gas exchanger, a pump, and a circulator.[69]

Among the light-based 3DP methods for fabricating microfluidic devices, most are centered on either directly fabricating the microfluidic features, or on producing master molds for PDMS microcasting. One of the relatively few MPP-3DP methods was reported by Lim et al., where a two-photon polymerization printer was used to fabricate a short, 3D "crossing manifold micromixer" directly from a two-photon crosslinkable resin.[70] With channel dimensions at 50 μm × 50 μm, and a series of horizontally and vertically aligned manifolds, the micromixer was designed to quickly mix two liquids, and indeed homogeneously distributed two fluids at 90% mixing efficiency within just 250 μm, or just five times the channel's width. Urrios et al. reported direct fabrication of millifluidic devices out of PEGDA-hydrogels, utilizing DLP-3DP to create optically transparent, cytocompatible, and serpentine channels 1 mm in width and 2 mm in height (**Figure 5**a).[71] Liu et al. recently demonstrated a combination passive mixer and

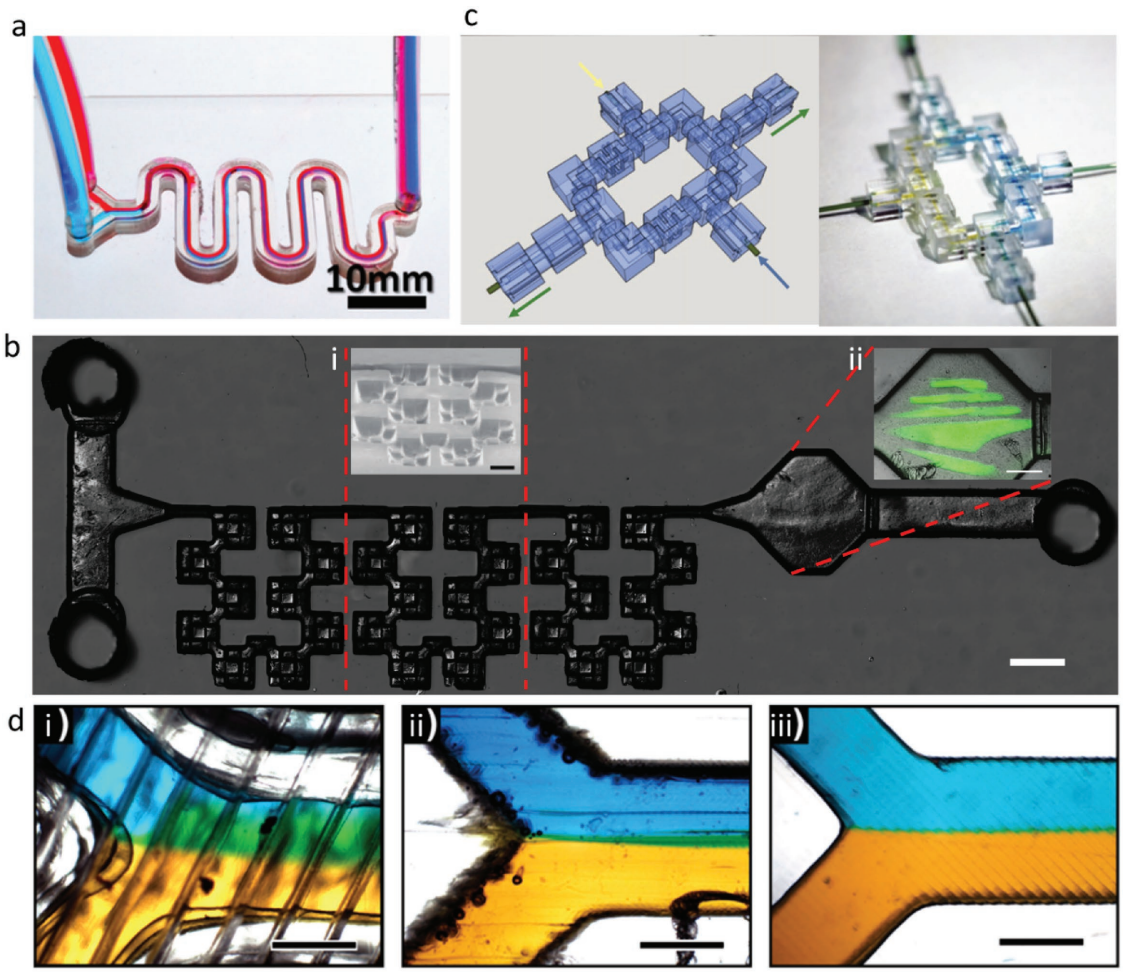

Figure 5. 3D-printing for microfluidics. a) Direct DLP-3DP of millifluidic serpentine channels in PEGDA hydrogels. Scale bar: 10 mm. Adapted with permission.[71] Copyright 2016, Royal Society of Chemistry. b) 3D passive mixer and biofabrication chamber, constructed via PDMS microcasting of a DLP-3D-printed master mold. Scale bar: 1 mm. i) inset: SEM image of mixing region, pitched at 45°. Scale bar: 500 µm. ii) Inset: biofabrication chamber, where 3D cell-laden constructs were printed. Scale bar: 500 µm. Adapted with permission.[72] Copyright 2016, Royal Society of Chemistry. c) Discrete, modularizable, and networkable microfluidic components for user-defined devices, fabricated via DLP-3DP. The example shown is a single-circuit mixer; left: 3D model; right: device in reality. Connectors are 1 mm in length, with fluidic cross sections at 750 µm in diameter. Adapted with permission.[74] Copyright 2014, The National Academy of Sciences. d) Comparison of Y-combinator straight-channel mixer, printed using: i) FDM, ii) MJM, and iii) DLP 3DP, respectively. Scale bars: 500 µm. Adapted with permission.[78] Copyright 2017, American Chemical Society.

cell-culture chamber, utilizing DLP-3DP to fabricate variable-height master molds out of PEGDA hydrogels, upon which PDMS microcasting was performed to create the final device (Figure 5b).[72] To demonstrate the device's utility, its variable height steps were used to passively mix gelatin methacrylate-based hydrogels and a fibroblastic cell line in a short length scale. Afterward, they utilized the noncontact nature of DLP-3DP to fabricate additional structures inside the already-completed device, with the optical transparency of the PDMS allowing direct photopolymerization of the cell-laden hydrogel inside the device's main chamber. Rogers et al. implemented DLP-3DP to produce microfluidic devices with integrated membrane-based valves,[73] with the valves containing horizontal, rectangular cross-sectional inlets and outlets as thin as 350 µm wide and 250 µm tall, in addition to vertical cylindrical control and flush ports with a diameter of 210 µm. The valves were demonstrated to work for up to 800 actuations. The ability to directly print the membrane-based valves onto glass enhances the likelihood of being able to include various substrates in printing, presenting the potential to lower the barrier-to-entry and aid in further research regarding lab-on-a-chip.

Microfluidic devices are often custom-built for a single application, and unless care is taken to generalize their design, they may have limited use in other applications. Combined with the fact that microfluidic-device production currently has a high cost-of-entry in terms of both skill and capital, there is interest in creating modularizable microfluidic components, for the sake of accessibility. Bhargava et al.,[74] Sochol et al.,[75] and Tsuda et al.[76] are all examples of groups utilizing 3D-printing to fabricate discrete, modular, and networkable microfluidic components, with the intention that any number of potential components can be mixed-and-matched at the end-users' discretion to create custom devices. As a more detailed example, Bhargava et al.'s study features

SLA-3D-printed fluidic components 1 mm in length and fluidic cross-sections 750 μm in diameter, with standardized inlets and outlets such that they can be fitted together to form a collective microfluidic device. They demonstrated reconfigurable and tunable microdroplet generators, as well as a passive mixing device (Figure 5c), with varying designs for each. Studies such as these aim to lay the groundwork for standardized "libraries" of microfluidic components, with the hope that advanced designs of high utility can be created easily by people who do not have the access, training, or time for cleanroom-grade micro-stereolithography.

There have been efforts to characterize the suitability of various 3D-printing types in fabricating microfluidic devices: if 3D-printers of different operating principles are tasked to make the same device, the resultant devices often will not be identical in form or function as an inherent consequence of the 3D-printers' operation. Lee et al. conducted a comparative study on MJM- and FDM-3DP capabilities in fabricating microfluidic rotational-flow devices and gradient generators, while also assessing parameters such as printer resolution, surface roughness, and biocompatibility.[77] As an example of comparative capability, they found that feature sizes under 100 μm were unattainable with both their MJM and FDM 3D-printers, but they were able to achieve a 5% accuracy rating for feature sizes above 500 and 1000 μm, respectively. Ultimately, they found that their chosen MJM 3D-printer was superior to that of their chosen FDM 3D-printer in terms of spatial accuracy, resolution, and smoothness across all three axes of motion, with an average deviation of 25.2 μm across all measurement series, as compared to 67.8 μm for the FDM; although they acknowledged that specialty tooling such as finer nozzles and motion controllers for their FDM 3D-printer could mitigate these shortcomings.

Macdonald et al. conducted a similar study, this time a direct comparison of their FDM, MJM, and DLP-based 3D-printers in fabricating a single, straight microfluidic channel—each of these were evaluated in the context of mixing efficiency of two flowing reagents (Figure 5d).[78] Their FDM printer produced the roughest surfaces as an inherent consequence of fusing large, circular filaments, but performed the best at mixing as a result (100% mixing within 15 mm of the inlet for all flow rates tested). Their DLP printer produced the smoothest features with the highest resolution, but, as a result, the microfluidic channel experienced a maximum mixing efficiency of only 32% at 25 mm from the inlet at 25 μL min^{-1}. Their MJM printer tread a middle-ground between the FDM and DLP 3D-printers—there was sidewall roughness in the channel due to the 16 μm layer size inherent to their MJM setup, but they were able to show 83% mixing at 25 mm from the inlet at 100 μL min^{-1} flow rates. While the authors cautioned championing any one modality as "the best," they did suggest optimum applications for each printing modality that took advantage of how each printer type inherently functioned: FDM 3D-printers would be well-suited for creating passive micromixers, or applications where mixing has no impact on the outcome; MJM 3D-printers would be optimal for complex geometries that do not require high precision; and DLP 3D-printers would be well suited for microfluidic applications where precise control of features and fluidics is critical.[78]

4. Discussion and Future Outlook

The rising popularity of 3D-printing in many sectors of the consumer and professional market has driven significant leaps in sophistication and capability. Such advances improve the ability to actualize challenging manufacturing ideas, and, as demonstrated here, have resulted in novel and functional biomedical microdevices. However, an important consideration is that device design can be highly situationally dependent, and, depending on the application, there are different 3D-printing limitations and challenges to be overcome, which can encompass parameters ranging from material workability and suitability to construction speed and print resolution (**Table 1**). We acknowledge that other reviews in the field have covered the technical minutiae of the capabilities of various 3D-printers;[3,5,32,33,66,79] instead, here we consider in a more general sense the concepts, limitations, and relative advantages/disadvantages that a potential 3D-printer user might consider important when selecting a particular modality for their specific application. Additionally, we discuss potential future directions that the field of 3D-printing functional biomedical microdevices may take.

4.1. Considerations in Selecting a 3D-Printing Modality

Fundamental to any given 3D-printer's operation is the ability to add and/or shape material in a precise manner, and any movement in 3D space necessitates fine control of whichever mechanisms performing the construction operations. While 3D-printing technology has improved immensely in recent years, tradeoffs still exist where one type of printer will excel in one domain compared to another.

4.1.1. Materials Selection

From a materials standpoint, 3D-printing technology has a large variety of materials to choose from, although the exact choice will differ depending material property suitability, and the specific application's requirements. Sometimes these choices can be constrained by the materials' workability, or economic costs in acquiring and/or modifying materials for use, while at other times, the choice is an inherent consequence of how different classes of 3D-printers are often optimized for a specific type or category of material, usually tied closely to the method by which the 3D-printer operates.

As an example, extrusion-based 3D-printers (E-3DPs) at their most fundamental, depend on the controlled release/deposition of material through a forming tool, whether that be a nozzle, dropper, or some other aperture. The method of forcing extrusion can vary as well, from the use of mechanical feeding, positive/negative pressure, and/or hydrostatic forces, but ultimately E-3DPs are restricted to materials capable of liquid-like flow, such as hydrogels, viscoelastics, and/or thermoplastic polymers. FDM 3D-printers, the more restricted counterpart to ordinary nozzle-based 3D-printers, would be limited to thermoplastic materials extruded through a heated forming nozzle. With most MJM 3D-printers on the market, such as the ones

Table 1. Feature comparison of E-3DP and L-3DP techniques in relation to functional biomedical microdevice fabrication.

Features	Extrusion-based 3D-printing (E-3DP)			Light-based 3D-printing (L-3DP)		
	Nozzle	FDM	MJM	SLA	MPP	DLP
Operating principle	Controlled deposition of flowable materials via nozzle	Filamentous deposition of thermoplastic polymers via nozzle	Deposition of crosslinkable polymers via inkjet heads	Raster-scanned laser photopolymerization of photosensitive substrates	Photopolymerization via nonlinear multiple photon absorption	2D cross-sectional photopolymerization of photosensitive substrates
X/Y Resolution	≈5–200 µm	≈5–200 µm	≈50 µm/100 s of DPI	Light-spot-dependent; can be sub-micrometer	Can defeat diffraction limit; sub-100 nm	Projected-pixel-size-dependent; can reach 1 µm
Speed	≈500 µm s^{-1} to 24 mm s^{-1}	≈sub-mm s^{-1} to 6 mm s^{-1}	≈1–40 mm s^{-1}	≈100s µm s^{-1} – several cm s^{-1}	≈80 nm s^{-1} to 2 cm s^{-1}	≈25–1000 mm min^{-1}
Advantages	Can utilize wide variety of materials, including biological	Tabletop form factor and cheap materials	May print multiple materials	Laser light enables high-resolution prints at reasonable speeds	Can produce much smaller structures compared to other L-3DP techniques	2D projection enables higher throughput compared to raster-scanning
	Print resolution limited by extrusion aperture and motion controller precision			Print resolution can suffer nonspecific photopolymerization due to light leakage into surrounding areas		
Limitations	Viscosity of substrate can impact nozzle performance	Circular cross-sections can prevent interfilament and interlayer fusion	Requires sacrificial support materials; removal can be difficult	Limited mainly to UV-sensitive resins; low throughput	Slow speeds limit larger-form-factor fabrication; costly equipment	Prints require large volumes of photopolymerizable; wasted material can become cost-prohibitive
References	[80,86,100–102]	[80,86,103,104]	[5,80,86,105]	[87,88,106–109]	[87–89,106–109]	[5,82,86]

available by the company Stratasys (CA, USA), their material choices are restricted in a similar fashion to that of nozzle-based and FDM 3D-printers, in that the build substrate must be flowable, but are unique in that the material must also be crosslinkable postdeposition, i.e., UV photopolymerizable in the case of Stratasys systems.

L-3DPs, such as DLW, MPP, and DLP-3D-printers all crucially depend solely on photopolymerization, and, as such, are limited to materials that are liquid, photosensitive, and transparent (or at least translucent). As most L-3DP methods happen in a build vat containing an excess of the photosensitive substrate, there is none of the selective deposition of materials to desired locations as with other E-3DP methods, raising an economic resource concern of wasting unpolymerized materials in the vat. Finally, in the context of biomedical applications, material biocompatibility is a key consideration—most solutions available on the commercial market are not optimized for biocompatibility, and often proprietary formulations make modifications difficult.[5] This sometimes requires users to come up with their own biocompatible materials, or resort to working with known biocompatible materials.

4.1.2. Resolution and Feature Size

From materials selection, we transition to resolution and feature-size considerations: E-3DPs, assuming that their extruded material does not experience postdeposition changes in size, are ultimately limited by the precision of their motion controllers and the physical size of their extrusion aperture(s), which in recent literature has reached a lower limit on the order of several microns for certain nonbiological microextrusion printers.[80] In general, this resolution stands to be improved if finer nozzle features and motion-control mechanisms are implemented. With FDM printers in particular, the nature of thermoplastically extruding large filaments means that: (i) the filament sizes can sometimes be larger than the sizes of the desired features, (ii) topologically, the filaments are round and can result in unwanted geometries, and (iii) the bonding between adjacent filaments (and thus adjacent layers) is mechanically weak, and thus prone to failures, leakages, and unwanted material properties. However, the advent of finer nozzle sizes and techniques for improving interfilament and interlayer fusion[81–83] have enabled easier fabrication of 3D constructs, and will only improve with time. Modern MJM-3DPs, such as those built by Stratasys (CA, USA), often specify resolution in terms of dots per inch (DPI) through arrays of nozzles just 50 µm in diameter,[84] but can suffer "smearing" at smaller feature sizes due to the action of a leveling device that smooths each layer after deposition.[85]

With L-3DP systems, resolution is ultimately determined by the spot size of the incident light, and in the case of free-radical photopolymerization, secondary consideration is given to the diffusion of free radicals outward from the irradiated zone. Focusing optics can be used to further shrink the spot size of the incident light—in the case of recent advances of DLP-3DP, resolutions of 1 µm can be achieved,[86] and, in the case of MPP-3DP, the diffraction limit can be overcome to achieve resolutions of less than 100 nm.[87–89] Additionally, as the build material is liquid and transparent (or at least translucent), there is potential for nonspecific photopolymerization to occur as light "leaks" deeper into the areas around the intended irradiation zone, which, in turn, further compounds the issue of unwanted free-radical polymerization. To mitigate

these issues, one potential solution might be to chemically modify the build material to include free-radical absorption and/or light-quenching molecules, e.g., Sudan I, 2-hydroxy-4-methoxy- benzophenon-5-sulfonic acid, or 2,2,6,6-tetramethylpiperidine 1-oxyl,[90,91] thus limiting the spread of nonspecific polymerization.

4.1.3. Speed and Throughput

In terms of speed and throughput, 3D-printing inherently involves the successive building of layers in 3D space, and how those individual layers are built can be loosely grouped into two paradigms: (i) serial printing, where each layer is formed drop-by-drop or line-by-line (e.g., nozzle/FDM-3DP, DLW-3DP) before moving on to the next layer; and (ii) parallel printing, where individual layers are fully formed whole before being joined to the next layers (e.g., MJM-3DP, DLP-3DP). Parallel printing can also encompass efforts to employ multiple serial mechanisms in tandem, such as utilizing more than one extruder in nozzle-based or FDM-3DP,[92] or multiple laser beams in SLA[93] or MPP-3DP[89] techniques.

3D-printers that operate in serial fashion must form every feature of a given layer before moving onto the next; thus, the total print speed is bottlenecked by how fast the printing mechanism can physically move while still retaining print fidelity. As examples, consider how FDM-3DP is limited both by how fast its printhead can traverse its motion of axes; going faster than the printer's ability to spool thermoplastic filament and/or faster than that which the extruded filament can handle during its postdeposition cooldown phase can negatively impact the print quality. SLA-3DP can raster-scan a laser very quickly across a resin's surface using mirror galvanometers, but is limited by the stop-and-go motion of its vertical stage as it passes from one layer to the next—some commercial SLA-3DPs have wipers that physically smooth the resin surface between every layer, further bottlenecking the print speed.[94] MPP-3DP systems can freely trace a laser in 3D space via mirror galvanometers, but the time required to produce high-resolution features increases cubically as a result of needing to raster-scan in three dimensions.[89] In terms of throughput, attempting to fabricate multiple objects in one build session using serial printing will increase the build time—assuming all of the devices fit within the 3D-printer's available build volume; this means that the printing mechanism(s) must now attend to each feature of a given layer for every additional device before it can begin to pass onto the next layer.

In contrasting serialized printing with parallel printing, entire 2D cross-sections can be formed at once in a single pass before moving onto the next layer. In MJM-3DP, parallel printing is achieved by virtue of having multiple printheads with many dispensing nozzles—an example of this is the Stratasys-built Objet500 Connex3,[84] where eight printheads of 96 nozzles each move in tandem to deposit tiny droplets of photocurable polymer at an X/Y resolution of 600 DPI. Provided the total footprint of the intended 3D object is not larger than the available footprint of the printhead architecture, a single pass can deposit an entire layer of features before moving onto the next layer. Combined with the ability to dispense multiple materials at controlled locations, MJM-3DP can create complex multimaterial 3D objects in a shorter timescale than their serialized counterparts. DLP-3D-printers, by virtue of being able to project an entire 2D light plane, are speed-limited mostly by the vertical movement of the stage responsible for moving the projected focal plane within the build volume, with secondary consideration for the substrate's photoinitiation efficiency. Faster movement of the stage will often decrease the build time, although this may be at the expense of the build quality and feature resolution.[19]

Many of the considerations discussed thus far are inextricably linked in compromise—larger and more complex objects will take more time to complete than smaller and simpler objects; build quality and feature resolution are often inversely proportional to speed; and attempting to print many objects may or may not slow the total build time, depending on the methodology used. By discussing some of the relative advantages/disadvantages associated with the 3D-printing techniques presented here, it is our hope that aspiring 3D-printer users have a better understanding of which techniques may best suit their specific application needs.

4.2. Future Outlook

Since the 2009 patent expiration on FDM-type 3D-printing, and the expiry of key stereolithography patents in 2014,[66] public awareness of 3D-printing has grown, bringing attention not only to the various technologies that comprise the field but also to their extensive manufacturing potential. 3D-printers of all kinds have become cheaper, smaller, and more sophisticated in the last decade, increasing public access and ease of production for the scientific, medical, and research communities. In the context of functional biomedical microdevices, 3D-printing represents a paradigm shift in manufacturing, as it significantly reduces the amount of time and resources spent in turning a conceptual idea into reality, compared to traditional techniques such as photolithography, subtractive manufacturing, or high-throughput injection molding. It becomes possible to rapidly prototype and iterate through designs on a small scale before committing resources to large-scale and costly manufacturing processes, thus advancing research and development on both data and economic fronts. The capability of 3D-printing with multimaterials also enables the one-step fabrication of microdevices with functional parts, potentially eliminating aspects of the traditional multistep manufacturing processes. For instance, in the context of microfluidic-device manufacturing, instead of separately constructing and assembling the tubes, valves, and chambers, the entire microfluidic device could be 3D-printed in one step, as well as other functional elements such as sensors and actuators, if the application requires them. In this way, 3D-printing makes the manufacturing of more complex and versatile biomedical devices possible.

We also consider a domain only lightly discussed in this work—the frontier of tissue-engineered systems, such as vasculature and disease models. Of the many goals of tissue engineering, two prominent goals are: (i) to produce tissues and organs that are of clinical-relevance for transplantation, and (ii) to create tissue-engineered models for investigation

of disease pathologies and/or pharmaceutical compound screening.[1] However, one of the fundamental limitations in producing clinical-scale tissues is the difficulty in producing functional vasculature—the diffusion limit of nutrient/waste transport in tissues is limited to the regime of 250 μm, and, as such, any larger-scale tissue-engineered constructs will critically require vascularization to maintain viability or be clinically relevant.[86] This scenario is where microfluidic devices may fill an important niche in tissue engineering, as vasculature and microfluidic channels are similar from a geometric and fluidic perspective.[95]

Producing biocompatible structures capable of supporting tissue-scale growth still remains an active area of research, as not all 3D-printing technologies support biocompatible materials, and fewer still are capable of producing vascularized tissues of meaningful utility. Existing methods for producing vasculature and tissue constructs vary greatly, from using sacrificial placeholders to directly printing negative spaces, but all invariably involve some manner of creating hollow, perfusable, biocompatible scaffolds in conjunction with cells of interest. Of the E-3DP and L-3DP methods described, several salient attempts at vascularization and tissue models have been reported: one example is Zhu et al.'s DLP-3DP fabrication of a multicellular, prevascularized tissue construct, where endothelial cells formed lumen-like structures in vitro, and host vasculature integration when implanted in vivo was successfully demonstrated.[96] Another is Ma et al.'s DLP-3DP-based fabrication of a liver tissue construct, where human-induced pluripotent stem-cell-derived hepatic progenitor cells and supportive cell types were spatially patterned into hexagonal patterns reminiscent of liver lobule architecture.[97] Yet another is Kolesky et al.'s utilization of a nozzle-based 3D-printer, where sacrificial hydrogels were embedded in a block of gelatin methacrylate, then flushed and perfused with endothelial cells[98]—this method was later scaled up for larger constructs on the order of 1 cm.[99] Efforts such as these signal a brighter future in the domain of functional biomedical microdevices, as greater strides in 3D-printing biologically compatible materials will further enhance medical healthcare technology, regenerative medicine, and pharmaceutical drug discovery.

5. Conclusions

The functional biomedical microdevices described here showcase the wide range of capabilities and types of devices that 3D-printing can produce, and we believe that technological progress in the 3D-printing domain is inevitable. We have seen the sheer range of applications that can be wrought, from micromachines and microfluidics to pharmaceuticals and biosensors. The capital cost, tooling, and maintenance requirements of 3D-printers of varying modalities shrink by the year, to the point where consumer-level desktop 3D-printers can be bought for recreational purposes. The fabrication capabilities of even consumer-grade 3D-printers can print features at the scale of tens of micrometers[94] with a wide variety of materials, and it is expected that both the cost and resolution of such printers will continue to shrink in the near future. The increasing popularity and decreasing cost of 3D printers will significantly increase its accessibility in both scientific research and industry to develop functional biomedical microdevices with less effort and better performance, at an accelerated yet economical pace. While we acknowledge that we have not covered all of the available technologies and capabilities of 3D-printing here, we can see from the work discussed from just this past decade that in the context of functional biomedical microdevice production, technological progress in 3D-printing has enabled creative and innovative studies to flourish. We see an exciting time ahead for the future of 3D-printing, and, as the various barriers from conception to production continue to be overcome, humanity's ability to advance research and development, bolster personalized healthcare, and improve the quality of life for all will continue to evolve.

Acknowledgements

This work was supported in part by grants from the California Institute for Regenerative Medicine (Grant No. RT3-07899), the National Institutes of Health (Grant Nos. R01EB021857 and R21HD090662), and the National Science Foundation (Grant Nos. CMMI 1547005 and CMMI-1644967).

Conflict of Interest

The authors declare no conflict of interest.

Keywords

3D-printing, biomedical, biomaterials, microdevices, microfluidics

Received: August 11, 2017
Revised: September 15, 2017
Published online: December 19, 2017

[1] C.-Y. Liaw, M. Guvendiren, *Biofabrication* **2017**, *9*, 24102.
[2] F. P. W. Melchels, J. Feijen, D. W. Grijpma, *Biomaterials* **2010**, *31*, 6121.
[3] B. C. Gross, J. L. Erkal, S. Y. Lockwood, C. Chen, D. M. Spence, *Anal. Chem.* **2014**, *86*, 3240.
[4] J. O'Donnell, M. Kim, H.-S. Yoon, *J. Manuf. Sci. Eng.* **2016**, *139*, 10801.
[5] N. Bhattacharjee, A. Urrios, S. Kang, A. Folch, *Lab Chip* **2016**, *16*, 1720.
[6] T. Billiet, M. Vandenhaute, J. Schelfhout, S. van Vlierberghe, P. Dubruel, *Biomaterials* **2012**, *33*, 6020.
[7] L. Novakova-Marcincinova, I. Kuric, *Manuf. Ind. Eng.* **2012**, *11*, 1338.
[8] H. N. Chia, B. M. Wu, *J. Biol. Eng.* **2015**, *9*, 4.
[9] C. W. Hull, US Patent 4575330 **1986**, 1.
[10] H. B. Sun, S. Kawata, *Adv. Polym. Sci.* **2004**, *170*, 169.
[11] M. Kaur, A. K. Srivastava, *J. Macromol. Sci. Part C: Polym. Rev.* **2002**, *42*, 481.
[12] S. F. S. Shirazi, S. Gharehkhani, M. Mehrali, H. Yarmand, H. S. C. Metselaar, N. Adib Kadri, N. A. A. Osman, *Sci. Technol. Adv. Mater.* **2015**, *16*, 33502.
[13] E. Stratakis, A. Ranella, M. Farsari, C. Fotakis, *Prog. Quantum Electron.* **2009**, *33*, 127.

[14] Y. Lu, G. Mapili, G. Suhali, S. Chen, K. Roy, *J. Biomed. Mater. Res., Part A* **2006**, *77*, 396.
[15] J. C. A. A. Bertsch, S. Zissi, J. Y. Jézéquel, S. Corbel, *Microsyst. Technol.* **1997**, *3*, 42.
[16] A. Bertsch, H. Lorenz, P. Renaud, *Sens. Actuators, A* **1999**, *73*, 14.
[17] L. Beluze, A. Bertsch, P. Renaud, *Proc. SPIE* **1999**, *3680,* 808.
[18] C. Sun, N. Fang, D. M. Wu, X. Zhang, *Sens. Actuators, A* **2005**, *121*, 113.
[19] J. R. Tumbleston, D. Shirvanyants, N. Ermoshkin, R. Janusziewicz, A. R. Johnson, D. Kelly, K. Chen, R. Pinschmidt, J. P. Rolland, A. Ermoshkin, E. T. Samulski, J. M. DeSimone, *Science* **2015**, *347*, 1349.
[20] E. M. Purcell, *Am. J. Phys.* **1977**, *45*, 1.
[21] S. Tottori, L. Zhang, F. Qiu, K. K. Krawczyk, A. Franco-Obregón, B. J. Nelson, *Adv. Mater.* **2012**, *24*, 811.
[22] T. Qiu, T.-C. Lee, A. G. Mark, K. I. Morozov, R. Münster, O. Mierka, S. Turek, A. M. Leshansky, P. Fischer, *Nat. Commun.* **2014**, *5*, 5119.
[23] C. Cvetkovic, R. Raman, V. Chan, B. J. Williams, M. Tolish, P. Bajaj, M. S. Sakar, H. H. Asada, M. T. A. Saif, R. Bashir, *Proc. Natl. Acad. Sci. USA* **2014**, *111*, 10125.
[24] W. Zhu, J. Li, Y. J. Leong, I. Rozen, X. Qu, R. Dong, Z. Wu, W. Gao, P. H. Chung, J. Wang, S. Chen, *Adv. Mater.* **2015**, *27*, 4411.
[25] M. Alomari, F. H. Mohamed, A. W. Basit, S. Gaisford, *Int. J. Pharm.* **2015**, *494*, 568.
[26] N. Scoutaris, M. R. Alexander, P. R. Gellert, C. J. Roberts, *J. Controlled Release* **2011**, *156*, 179.
[27] A. Goyanes, A. B. M. Buanz, G. B. Hatton, S. Gaisford, A. W. Basit, *Eur. J. Pharm. Biopharm.* **2015**, *89*, 157.
[28] J. Skowyra, K. Pietrzak, M. A. Alhnan, *Eur. J. Pharm. Sci.* **2015**, *68*, 11.
[29] S. A. Khaled, J. C. Burley, M. R. Alexander, J. Yang, C. J. Roberts, *J. Controlled Release* **2015**, *217*, 308.
[30] A. Goyanes, J. Wang, A. Buanz, R. Martinez-Pacheco, R. Telford, S. Gaisford, A. W. Basit, *Mol. Pharm.* **2015**, *12*, 4077.
[31] S. A. Khaled, J. C. Burley, M. R. Alexander, C. J. Roberts, *Int. J. Pharm.* **2014**, *461*, 105.
[32] L. K. Prasad, H. Smyth, *Drug Dev. Ind. Pharm.* **2016**, *42*, 1019.
[33] J. Goole, K. Amighi, *Int. J. Pharm.* **2016**, *499*, 376.
[34] I. D. Ursan, L. Chiu, A. Pierce, *J. Am. Pharm. Assoc.* **2013**, *53*, 136.
[35] M. A. Alhnan, T. C. Okwuosa, M. Sadia, K. W. Wan, W. Ahmed, B. Arafat, *Pharm. Res.* **2016**, *33*, 1817.
[36] Spritam, https://www.spritam.com (accessed: July 2017).
[37] N. G. Rouphael, M. Paine, R. Mosley, S. Henry, D. V. McAllister, H. Kalluri, W. Pewin, P. M. Frew, T. Yu, N. J. Thornburg, S. Kabbani, L. Lai, E. V. Vassilieva, I. Skountzou, R. W. Compans, M. J. Mulligan, M. R. Prausnitz, A. Beck, S. Edupuganti, S. Heeke, C. Kelley, W. Nesheim, *Lancet* **2017**, *390*, 649.
[38] Y. C. Kim, J. H. Park, M. R. Prausnitz, *Adv. Drug Delivery Rev.* **2012**, *64*, 1547.
[39] Y. Nir, A. Paz, E. Sabo, I. Potasman, *Am. J. Trop. Med. Hyg.* **2003**, *68*, 341.
[40] J. G. Hamilton, *J. Fam. Pract.* **1995**, *41*, 169.
[41] S. Indermun, R. Luttge, Y. E. Choonara, P. Kumar, L. C. Du Toit, G. Modi, V. Pillay, *J. Controlled Release* **2014**, *185*, 130.
[42] J. Li, M. Zeng, H. Shan, C. Tong, *Curr. Med. Chem.* **2017**, *24*, 2413.
[43] A. Ovsianikov, B. Chichkov, P. Mente, N. A. Monteiro-Riviere, A. Doraiswamy, R. J. Narayan, *Int. J. Appl. Ceram. Technol.* **2007**, *4*, 22.
[44] J. S. Kochhar, S. Zou, S. Y. Chan, L. Kang, *Int. J. Nanomed.* **2012**, *7*, 3143.
[45] S. H. Lim, J. Y. Ng, L. Kang, *Biofabrication* **2017**, *9*, 15010.
[46] S. P. Mohanty, E. Koucianos, *IEEE Potentials* **2006**, *25*, 35.
[47] Y. Zhang, S. Ge, J. Yu, *TrAC, Trends Anal. Chem.* **2016**, *85*, 166.
[48] G. W. Bishop, J. E. Satterwhite-Warden, K. Kadimisetty, J. F. Rusling, *Nanotechnology* **2016**, *27*, 284002.
[49] S. A. N. Gowers, V. F. Curto, C. A. Seneci, C. Wang, S. Anastasova, P. Vadgama, G. Z. Yang, M. G. Boutelle, *Anal. Chem.* **2015**, *87*, 7763.
[50] R. D. Boehm, P. Jaipan, K.-H. Yang, T. N. Stewart, R. J. Narayan, *Int. J. Bioprint.* **2016**, *2*, 1.
[51] A. Roda, M. Guardigli, D. Calabria, M. M. Calabretta, L. Cevenini, E. Michelini, *Analyst* **2014**, *139*, 6494.
[52] L. Cevenini, M. M. Calabretta, G. Tarantino, E. Michelini, A. Roda, *Sens. Actuators, B* **2016**, *225*, 249.
[53] P. R. Miller, S. D. Gittard, T. L. Edwards, D. A. M. Lopez, X. Xiao, D. R. Wheeler, N. A. Monteiro-Riviere, S. M. Brozik, R. Polsky, R. J. Narayan, *Biomicrofluidics* **2011**, *5*, 13415.
[54] K. Kim, W. Zhu, X. Qu, C. Aaronson, W. R. McCall, S. Chen, D. J. Sirbuly, *ACS Nano* **2014**, *8*, 9799.
[55] M. Gou, X. Qu, W. Zhu, M. Xiang, J. Yang, K. Zhang, Y. Wei, S. Chen, *Nat. Commun.* **2014**, *5*, 3774.
[56] C. A. Mandon, L. J. Blum, C. A. Marquette, *Anal. Chem.* **2016**, *88*, 10767.
[57] S. Stassi, E. Fantino, R. Calmo, A. Chiappone, M. Gillono, D. Scaiola, C. F. Pirri, C. Ricciardi, A. Chiado, I. Roppolo, *ACS Appl. Mater. Interfaces* **2017**, *9*, 19193.
[58] E. C. Spivey, B. Xhemalce, J. B. Shear, I. J. Finkelstein, *Anal. Chem.* **2014**, *86*, 7406.
[59] A. K. Au, W. Lee, A. Folch, *Lab Chip* **2014**, *14*, 1294.
[60] C. M. B. Ho, S. H. Ng, K. H. H. Li, Y.-J. Yoon, *Lab Chip* **2015**, *15*, 3627.
[61] S. Waheed, J. M. Cabot, N. P. Macdonald, T. Lewis, R. M. Guijt, B. Paull, M. C. Breadmore, *Lab Chip* **2016**, *16*, 1993.
[62] A. A. Yazdi, A. Popma, W. Wong, T. Nguyen, Y. Pan, J. Xu, *Microfluid. Nanofluid.* **2016**, *20*, 1.
[63] A. J. L. Morgan, L. H. San Jose, W. D. Jamieson, J. M. Wymant, B. Song, P. Stephens, D. A. Barrow, O. K. Castell, *PLoS One* **2016**, *11*, e0152023.
[64] G. W. Bishop, J. E. Satterwhite, S. Bhakta, K. Kadimisetty, K. M. Gillette, E. Chen, J. F. Rusling, *Anal. Chem.* **2015**, *87*, 5437.
[65] Dolomite Microfluidics, http://www.dolomite-microfluidics.com/ (accessed: July 2017).
[66] A. K. Au, W. Huynh, L. F. Horowitz, A. Folch, *Angew. Chem., Int. Ed.* **2016**, *55*, 3862.
[67] J. L. Erkal, A. Selimovic, B. C. Gross, S. Y. Lockwood, E. L. Walton, S. McNamara, R. S. Martin, D. M. Spence, *Lab Chip* **2014**, *14*, 2023.
[68] S. Begolo, D. V. Zhukov, D. A. Selck, L. Li, R. F. Ismagilov, *Lab Chip* **2014**, *14*, 4616.
[69] A. Causier, G. Carret, C. Boutin, T. Berthelot, P. Berthault, *Lab Chip* **2015**, *15*, 2049.
[70] T. W. Lim, Y. Son, Y. J. Jeong, D.-Y. Yang, H.-J. Kong, K.-S. Lee, D.-P. Kim, *Lab Chip* **2011**, *11*, 100.
[71] A. Urrios, C. Parra-Cabrera, N. Bhattacharjee, A. M. Gonzalez-Suarez, L. G. Rigat-Brugarolas, U. Nallapatti, J. Samitier, C. A. DeForest, F. Posas, J. L. Garcia-Cordero, A. Folch, *Lab Chip* **2016**, *16*, 2287.
[72] J. Liu, H. H. Hwang, P. Wang, G. Whang, S. Chen, *Lab Chip* **2016**, *16*, 1430.
[73] C. I. Rogers, K. Qaderi, A. T. Woolley, G. P. Nordin, *Biomicrofluidics* **2015**, *9*, 16501.
[74] K. C. Bhargava, B. Thompson, N. Malmstadt, D. Szuromi, D. F. Voss, J. I. Brauman, P. Szuromi, *Proc. Natl. Acad. Sci. USA* **2014**, *111*, 15013.
[75] R. D. Sochol, E. Sweet, C. C. Glick, S. Venkatesh, A. Avetisyan, K. F. Ekman, A. Raulinaitis, A. Tsai, A. Wienkers, K. Korner, K. Hanson, A. Long, B. J. Hightower, G. Slatton, D. C. Burnett, T. L. Massey, K. Iwai, L. P. Lee, K. S. J. Pister, L. Lin, *Lab Chip* **2016**, *16*, 668.

[76] S. Tsuda, H. Jaffery, D. Doran, M. Hezwani, P. J. Robbins, M. Yoshida, L. Cronin, *PLoS One* **2015**, *10*, e0141640.
[77] J. M. Lee, M. Zhang, W. Y. Yeong, *Microfluid. Nanofluid.* **2016**,*20*, 1.
[78] N. P. Macdonald, J. M. Cabot, P. Smejkal, R. M. Guijt, B. Paull, M. C. Breadmore, *Anal. Chem.* **2017**, *89*, 3858.
[79] M. Vaezi, H. Seitz, S. Yang, *Int. J. Adv. Manuf. Technol.* **2013**, *67*, 1721.
[80] S. V. Murphy, A. Atala, *Nat. Biotechnol.* **2014**, *32*, 773.
[81] S. Shaffer, K. Yang, J. Vargas, M. A. Di Prima, W. Voit, *Polymer* **2014**, *55*, 5969.
[82] J. W. Stansbury, M. J. Idacavage, *Dent. Mater.* **2016**, *32*, 54.
[83] E. J. McCullough, V. K. Yadavalli, *J. Mater. Process. Technol.* **2013**, *213*, 947.
[84] Stratasys Objet350–500 Connex3, http://www.stratasys.com/3d-printers/objet-350-500-connex3 (accessed: July 2017).
[85] Y. L. Yap, C. Wang, S. L. Sing, V. Dikshit, W. Y. Yeong, J. Wei, *Precis. Eng.* **2016**, *50*, 275.
[86] W. Zhu, X. Ma, M. Gou, D. Mei, K. Zhang, S. Chen, *Curr. Opin. Biotechnol.* **2016**, *40*, 103.
[87] S. Maruo, *Nippon GOMU KYOKAISHI* **2014**, *3*, 382.
[88] S. Maruo, O. Nakamura, S. Kawata, *Opt. Lett.* **1997**, *22*, 132.
[89] S. D. Gittard, A. Nguyen, K. Obata, A. Koroleva, R. J. Narayan, B. N. Chichkov, *Biomed. Opt. Express* **2011**, *2*, 3167.
[90] M. P. Lee, G. J. T. Cooper, T. Hinkley, G. M. Gibson, M. J. Padgett, L. Cronin, *Sci. Rep.* **2015**, *5*, 9875.
[91] A. P. Zhang, X. Qu, P. Soman, K. C. Hribar, J. W. Lee, S. Chen, S. He, *Adv. Mater.* **2012**, *24*, 4266.
[92] M. H. Ali, N. Mir-Nasiri, W. L. Ko, *Int. J. Adv. Manuf. Technol.* **2016**, *86*, 999.
[93] C. Jiang, *Rapid Prototyping J.* **2011**, *17*, 148.
[94] Autodesk Ember, https://ember.autodesk.com (accessed: July 2017).
[95] J. Tien, *Curr. Opin. Chem. Eng.* **2014**, *3*, 36.
[96] W. Zhu, X. Qu, J. Zhu, X. Ma, S. Patel, J. Liu, P. Wang, C. S. E. Lai, M. Gou, Y. Xu, K. Zhang, S. Chen, *Biomaterials* **2017**, *124*, 106.
[97] X. Ma, X. Qu, W. Zhu, Y.-S. Li, S. Yuan, H. Zhang, J. Liu, P. Wang, C. S. E. Lai, F. Zanella, G.-S. Feng, F. Sheikh, S. Chien, S. Chen, *Proc. Natl. Acad. Sci. USA* **2016**, *113*, 2206.
[98] D. B. Kolesky, R. L. Truby, A. S. Gladman, T. A. Busbee, K. A. Homan, J. A. Lewis, *Adv. Mater.* **2014**, *26*, 3124.
[99] D. B. Kolesky, K. A. Homan, M. A. Skylar-Scott, J. A. Lewis, *Proc. Natl. Acad. Sci. USA* **2016**, *113*, 3179.
[100] B. N. Johnson, K. Z. Lancaster, I. B. Hogue, F. Meng, Y. L. Kong, L. W. Enquist, M. C. McAlpine, *Lab Chip* **2015**, *16*, 1393.
[101] D. W. Hutmacher, M. Sittinger, M. V. Risbud, *Trends Biotechnol.* **2004**, *22*, 354.
[102] J. T. Muth, D. M. Vogt, R. L. Truby, Y. Mengüç, D. B. Kolesky, R. J. Wood, J. A. Lewis, *Adv. Mater.* **2014**, *26*, 6307.
[103] A. Goyanes, A. B. M. Buanz, A. W. Basit, S. Gaisford, *Int. J. Pharm.* **2014**, *476*, 88.
[104] N. N. Zein, I. A. Hanouneh, P. D. Bishop, M. Samaan, B. Eghtesad, C. Quintini, C. Miller, L. Yerian, R. Klatte, *Liver Transplant.* **2013**, *19*, 1304.
[105] Z. Bin, S. Baekhoon, N. VuDat, B. Doyoung, *J. Micromech. Microeng.* **2016**, *26*, 25015.
[106] G. Kumi, C. O. Yanez, K. D. Belfield, J. T. Fourkas, *Lab Chip* **2010**, *10*, 1057.
[107] Y. L. Zhang, Q. D. Chen, H. Xia, H. B. Sun, *Nano Today* **2010**, *5*, 435.
[108] N. Fang, C. Sun, X. Zhang, *Appl. Phys. A: Mater. Sci. Process.* **2004**, *79*, 1839.
[109] A. Selimis, V. Mironov, M. Farsari, *Microelectron. Eng.* **2014**, *132*, 83.